Available online at www.sciencedirect.com
ScienceDirect
Geothermics 37 (2008) 189–210
GEOTHERMICS
www.elsevier.com/locate/geothermics

Low-temperature geothermal potential of the flooded Gaspé Mines, Québec, Canada

Jasmin Raymond *, René Therrien

Département de Géologie et de Génie Géologique, Université Laval, Ste-Foy, Québec, Canada G1K 7P4

Received 5 October 2006; accepted 25 September 2007
Available online 17 March 2008

Abstract

The low-temperature geothermal potential of the flooded Gaspé Mines, near Murdochville, Québec, Canada, has been estimated from a long-term pumping test and numerical groundwater flow modelling. A former mining shaft was used to pump water for 3 weeks at a rate averaging 0.062 m^3/s (3720 L/min). A mean recovery temperature equal to 6.7 °C and a maximum drawdown of 3.63 m were observed during this test. The observed drawdown was reproduced with a three-dimensional finite element model that simulates groundwater flow through the mine workings and surrounding rock mass. The model was then used to simulate longer-term pumping performed for heat recovery. Modelling results combined with a simplified energy balance calculation suggest that a sustainable energy extraction rate is attained at a pumping rate of 0.049 m^3/s (2940 L/min), with a corresponding geothermal energy production potential of 765 kW, assuming a return water temperature of 3 °C. This energy could be extracted with heat pumps and used for space heating at the town's industrial park.

Keywords: Low-temperature geothermal resources; Mine water; Heat pump; Pumping test; Modelling; Gaspé Mines; Québec; Canada

1. Introduction

Deep flooded underground mines constitute potential low-temperature geothermal reservoirs that can be used for energy storage and production. Groundwater rebound following mine dewatering supplies water to flood workings (Adams and Younger, 2001) and transports the energy released by earth's natural heat flux and mineral oxidation (Ghomshei and Meech,

* Corresponding author. Tel.: +1 418 656 2131; fax: + 1 418 656 7339.
E-mail address: jasmin.raymond.1@ulaval.ca (J. Raymond).

0375-6505/$30.00 © 2007 Elsevier Ltd. All rights reserved.
doi:10.1016/j.geothermics.2007.10.001

Nomenclature

Cp	specific heat capacity [$L^2\,t^{-2}\,T^{-1}$]
E_c	captured thermal energy rate [$L^2\,M\,t^{-3}$]
E_{hp}	extractable thermal energy rate from water using heat pumps [$L^2\,M\,t^{-3}$]
E_r	thermal energy resources [$L^2\,M\,t^{-2}$]
g	gravitational acceleration [$L\,t^{-2}$]
h	hydraulic head [L]
h_{we}	hydraulic head at the well screen [L]
k	permeability tensor [L^2]
K	hydraulic conductivity [$L\,t^{-1}$]
K_{we}	hydraulic conductivity of a well [$L\,t^{-1}$]
L_s	total length of the well screen [L]
n	porosity
pH_s	saturation pH for calcium carbonate
P_{we}	wetted perimeter of the well [L]
q	fluid flux [$L\,t^{-1}$]
q_{we}	well fluid flux [$L\,t^{-1}$]
Q	pumping rate [$L^3\,t^{-1}$]
r_c	well casing radius [L]
r_s	well screen radius [L]
S_s	specific storage coefficient [L^{-1}]
T_p	pumped water temperature [T]
T_r	heat exchanger return water temperature [T]
V	water volume [L^3]
z	average depth [L]

Greek letters

α	geothermal gradient [$T\,L^{-1}$]
Γ_{bo}	fluid exchange rate between subsurface domain and boundaries [$L^3\,L^{-3}\,t^{-1}$]
Γ_{we}	fluid exchange rate between subsurface domain and wells [$L^3\,L^{-3}\,t^{-1}$]
λ	thermal conductivity [$L\,M\,t^{-3}\,T^{-1}$]
μ_w	water viscosity [$M\,L^{-1}\,t^{-1}$]
ρ	density [$M\,L^{-3}$]

Subscripts

b	bulk
s	solid
w	water

2003). Compared to the surrounding rock mass, former mine conduits form a very permeable system that can be used to recover mine water at potentially high pumping rates and extract its geothermal energy using heat pump technology (Huttrer, 1997). Mine water is a source of renewable energy that can contribute to the reduction of greenhouse gas emissions, thus representing an environmental benefit in contrast to the negative impacts generally associated with mine water chemistry (Banks et al., 1997).

It was the slight increase in temperatures in coal mines caused by coal oxidation that initially stimulated interest in extracting energy from mine water. A factory in the town of Springhill, Nova Scotia, Canada, has indeed been successfully doing so since 1989. Groundwater at 18 °C is recovered from the Springhill coal mine and used to heat and cool industrial buildings with heat pumps (Jessop et al., 1995). Energy is also being extracted from coal mine water at Shettleston and Lumphinnans in Scotland, UK (John Gilbert Architects, 2006a,b). Base-metal mine water was used with a heat pump system to heat and cool a municipal building near the Park Hills lead mine in Missouri, USA, in 1995 (Geothermal Heat Pump Consortium, 1997). Other coal and base-metal mines in Europe and North America with potential for energy extraction have been studied by Malolepszy et al. (2005), Raymond and Therrien (2006), Watzlaf and Ackman (2006), and Tóth and Bobok (2007). These examples demonstrate that the groundwater in most of these mine geothermal reservoirs can provide heat to local communities. Additional studies are, however, required at flooded mines to develop methods able to assess the energy production potential and also investigate the long-term impact of energy extraction on the hydrogeological and thermal regimes of these systems.

The recent closure of the mines and smelter in Murdochville, Québec, Canada, has provided an opportunity for the local municipality to explore its geothermal resources. In this paper we describe an assessment of the geothermal energy extraction potential of the flooded Gaspé Mines reservoir. A long-term pumping test in a former mining shaft and numerical groundwater flow simulations were used to estimate the energy attainable from mine water and to determine the geothermal potential of the site by means of an energy balance calculation. We also include the results of an independent economic assessment. Compared to previous case studies that focused on general concepts and resource estimates from mine water volume (Jessop et al., 1995; Watzlaf and Ackman, 2006), this study aims at a more detailed definition of the hydraulic properties of the mine workings. The methodology and results of the site characterisation, the pumping test analysis and the groundwater flow modelling are reported here to provide guidelines for further studies.

2. Site description and characterization

The former Gaspé Mines are located in a mountainous region in the middle of the Gaspé Peninsula near the town of Murdochville, at a latitude of about 49° North (Fig. 1). The mean air temperature at Murdochville is 1.6 °C and the average yearly precipitation is 1118 mm (Environment Canada, 2000). Copper porphyry and skarn mineral deposits were exploited at the mine from 1951 to 1999. During mining operations, the Needle Mountain and the Copper Mountain open pits and the three main underground zones, B, C and E, were excavated in the Early Devonian Gaspé Superior Limestone Group. More than 47 million tonnes of rock were mined from the three underground zones at depths ranging from 100 to 700 m.

The mine workings are located on the north flank of a NE–SW anticline that dips 15–35° north (Wares and Berger, 1995). The stratigraphy of the mine site is described in Allcock (1982), Bernard and Procyshyn (1992), Wares and Berger (1993) and Wares and Brisebois (1998). Rock formations, part of the Gaspé Superior Limestone Group, consist of calcareous mudstones and argillaceous limestones. Mudstones of the Indian Cove Formation, with thicknesses greater than 150 m, overlie a 110–160 m sequence of mudstone and 30–45 m of limestone from the Ship Head Formation. A 170–205 m thick mudstone unit, followed by 10–20 m of limestone and more than 490 m of mudstone from the Forillon Formation, underlie the Ship Head Formation. Porphyritic

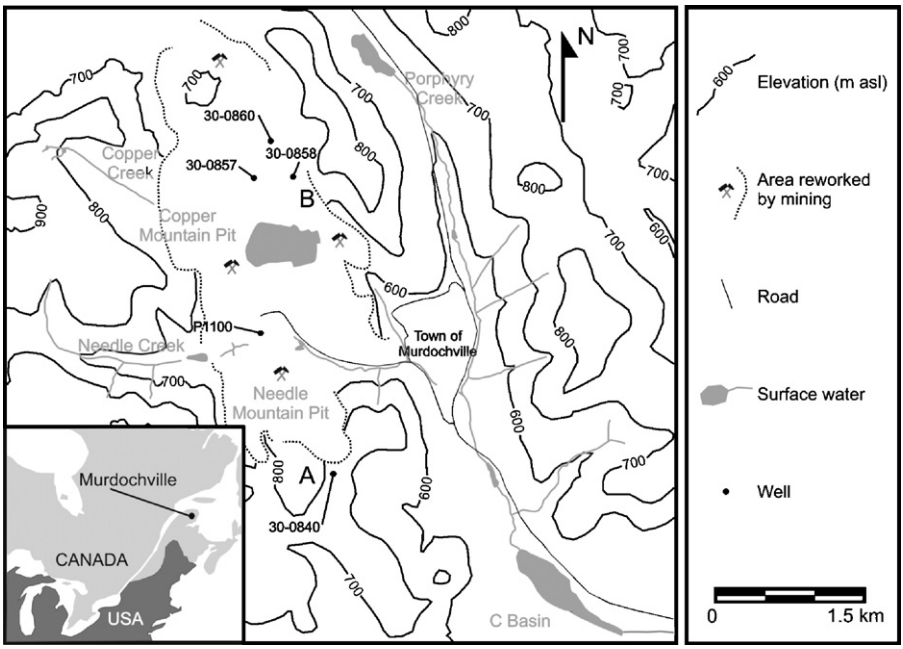

Fig. 1. Simplified topographical map of the Gaspé Mines area, showing location of the town of Murdochville. (A) and (B) denote the approximate location of the schematic cross-section in Fig. 2.

granodiorite intrusions crosscut the stratigraphic sequence to the north of the mine site. The host rock was metamorphosed by a felsic intrusion and altered by hydrothermal fluids. For this study, rock units with similar assumed hydraulic and thermal properties were grouped into five hydrostratigraphic units, U1 to U5; a schematic cross-section showing these units along with their physical properties is given in Fig. 2.

The main surface water bodies near the former mine are the copper, needle and Porphyry creeks, all flowing south. A few 60-mm diameter, diamond-drilled exploration boreholes were located (Fig. 1) and used to measure groundwater levels. Additional water level measurements were collected in the Copper Mountain Pit and in the former mining shaft P1100 to map the elevation of the water table; both are shown in Fig. 3. At the site, groundwater generally flows from elevated areas towards the Copper Mountain Pit, where the water level was approximately 539 m above sea level (m asl) at the time of this study (2005–2006).

Extensive pumping during almost 50 years of mining has lowered the water table around the mine. For example, groundwater was pumped out of the mine at an average rate of 0.219 m^3/s (13,140 L/m) during the last years of exploitation, with the rate tripling during snowmelt in the spring (Morin, 1992). Since mine closure, pumping has stopped and the water table has been rising but has not yet recovered its original elevation. In 2005–2006, the water level in the Copper Mountain Pit was still steadily rising.

2.1. Mine workings

The underground mine workings (Fig. 3) are described in Morin (1992) and Geocon (1994). The B zone has been mined in the mudstones of the Indian Cove Formation by the room-and-pillar

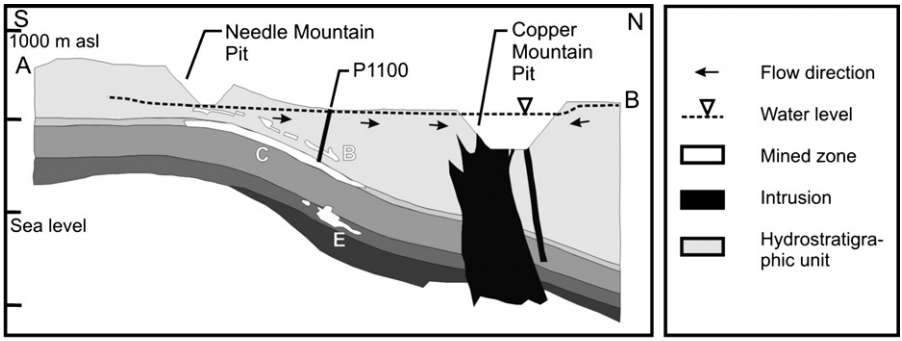

Hydrostratigraphy

Color	Unit	Corresponding rock formation	Dominant rock type	Mineralogy (wt%)* Qz	Ca	Ab-Mi	n**	λ_b [W/(m K)]	Cp_b [J/(Kg K)]
	U1	ICove-SHead	C-mudstone	60	15	25	0.05	4.77	792
	U2	SHeap	A-limestone	30	30	40	0.1	3.36	872
	U3	Forillon	C-mudstone	50	20	30	0.05	4.33	794
	U4	Forillon	A-limestone	20	40	40	0.1	3.12	879
	U5	Forillon	C-mudstone	60	20	20	0.05	4.87	797

Fig. 2. Schematic cross-section of the Gaspé Mines showing hydrostratigraphy and mine workings (section redrawn from Bernard and Procyshyn, 1992). Approximate location of (A) and (B) is shown in Fig 1. White colour (B), (C) and (E) denote underground working sections. ICove: Indian Cove Formation; SHeap: Ship Head Formation; A-limestone: argillaceous limestone; C-mudstone: calcareous mudstone; Qz: quartz; Ca: calcite; Ab-Mi: albite-microcline. *Average mineralogy inferred from geochemical data (Wares and Berger, 1993). **Porosity estimated on the basis of the rock type classification proposed by Freeze and Cherry (1979).

method and is divided into two sections: B-east and B-central. The former is located at depths of 80–120 m below surface to the east, and the latter is at about 50 m depth under the Needle Mountain Pit. The B-central section is not flooded since its elevation (650 m asl) is above the water table elevation in this area.

The C zone workings have been excavated in the limestones of the Ship Head Formation by both the room-and-pillar and the longhole-with-backfill methods. They are divided in the C-central and C-northwest sections, which are located at 180–500 m depth (between 520 and 100 m asl) under the B zone and towards the Copper Mountain Pit. The C-central section is large and continuous; it is of tabular form and dips north at about 23°. Both sections of the C zone are now totally flooded.

The E zone has been mined in the limestones of the Forillon Formation by the longhole method with backfill. It is divided in four sections, E-29, E-32, E-34 and E-38, which are located at depths of more than 580 m (below 20 m asl) beneath the town of Murdochville. Each section has been mined for a specific ore deposit. All E zone sections are interconnected and communicate with the C zone by underground roads. The E zone is now completely flooded.

All mining shafts and underground roads that used to connect the workings of zones B and C to the surface were blocked with backfill and/or cement caps at mine closure. Some of these shafts and roads could, however, be re-opened and used as conventional water wells to pump out mine water at high rates.

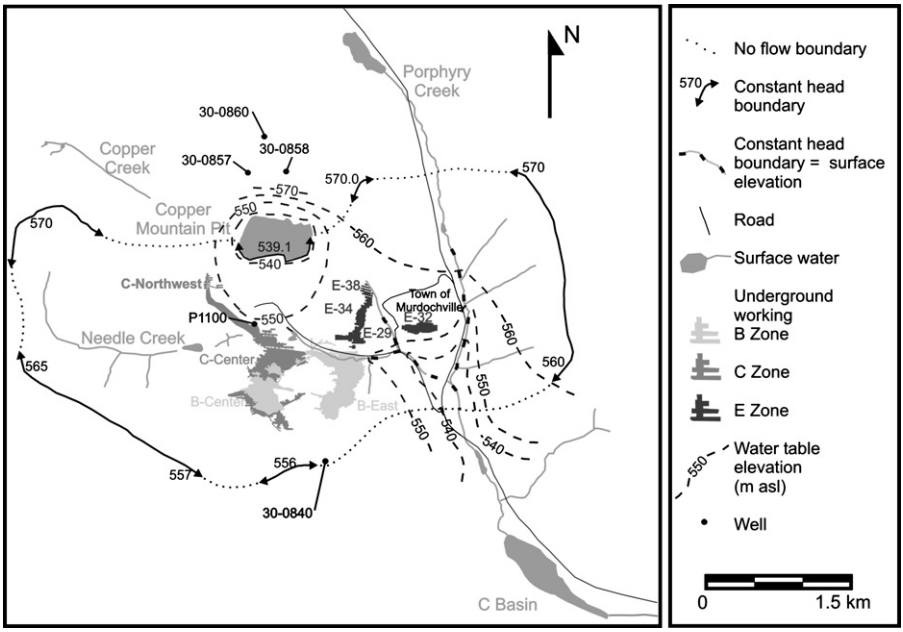

Fig. 3. Map showing the area above the mine workings, the water table elevations and boundaries used in the groundwater flow model.

2.2. Thermal properties, heat flux and energy resources

The thermal properties of the hydrostratigraphic units shown in Fig. 2 had to be estimated from petrographic descriptions and the chemical composition of the rock units. These estimates were made using inferred mineral contents and porosity values (n) assigned to each of these units on the basis of the rock type classification proposed by Freeze and Cherry (1979). The weight percent of the main mineral phases (quartz, calcite and albite-microcline) was inferred using geochemical data reported by Wares and Berger (1993). The bulk thermal conductivity (λ_b) of each rock unit was calculated using (Brailsford and Major, 1964):

$$\lambda_b = \lambda_s \frac{X - 2nY}{X + nY} \tag{1}$$

where

$$X = 2a + 1 \tag{2}$$

$$Y = a - 1 \tag{3}$$

and

$$a = \frac{\lambda_s}{\lambda_w} \tag{4}$$

The geometric average of the mineral thermal conductivities was calculated from the main mineral phases to determine the bulk thermal conductivity of the solids (λ_s). The water and mineral thermal conductivities were taken from Chemical Rubber Company (2006) and Clauser

and Huenges (1995). The bulk specific heat capacity (Cp_b) of each unit was computed from (Waples and Waples, 2004b):

$$Cp_b = \frac{\rho_s Cp_s(1-n) + \rho_w Cp_w n}{\rho_b} \quad (5)$$

In Eq. (5), the specific heat capacity of the solids (Cp_s) was calculated as the weighted average of the specific heat capacity of the main mineral phases. The water and mineral specific heat capacities were obtained from Somerton (1992) and Waples and Waples (2004a), and the solid density (ρ_s) of each unit was estimated from the inferred mineralogy. The water density (ρ_w) was assumed equal to 1000 kg/m^3 and the bulk density (ρ_b) was calculated from the porosity-weighted average of solid and water densities.

Temperature profiles (Fig. 4) were measured in four exploration holes to a depth of 300 m with a thermistor, using an ACR Nautilus 85 logger having a precision of 0.4 °C. The upper sections of these profiles show seasonal temperature variations and the lower sections indicate an average geothermal gradient of 0.011 °C/m. This value is similar to the 0.0131 °C/m obtained by Drury et al. (1987) when measuring the heat flux in a deep borehole near Murdochville. The local gradient, below the worldwide average of 0.02–0.03 °C/m, may be partly the result of lateral groundwater flow.

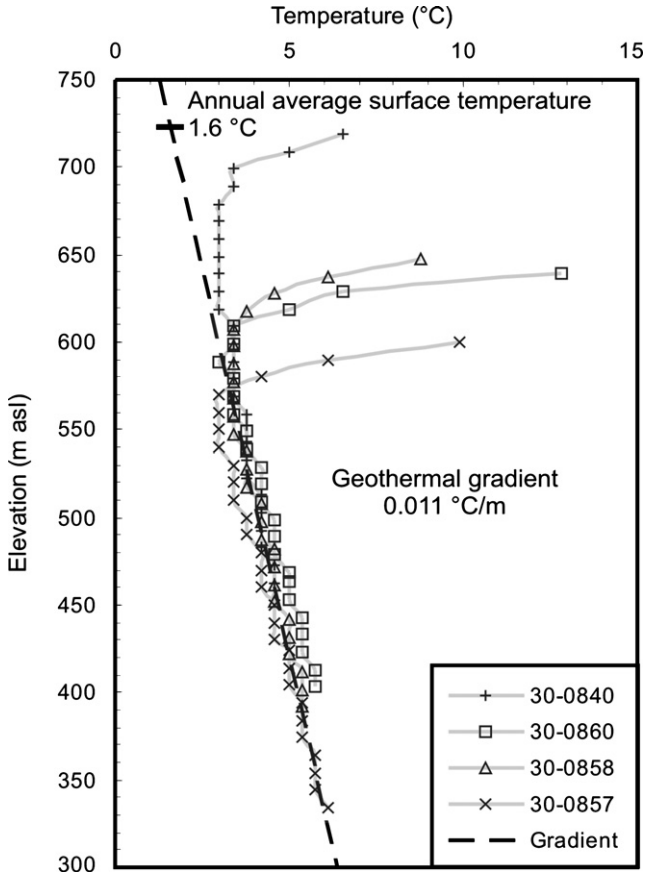

Fig. 4. Temperature profiles measured in four exploration holes (see Fig. 3 for their location).

The surface heat flux on-site was estimated by multiplying the geothermal gradient (0.011 °C/m) by the global thermal conductivity, assumed equal to 4.67 W/mK. That global value is the geometric average of the bulk thermal conductivities estimated from the mineralogy of the hydrostratigraphic units. The estimated surface heat flux is therefore equal to 51 mW/m^2, while the measurements by Drury et al. (1987) gave a value of 50 mW/m^2. Note that there is no heat flow map available for the Gaspé region but these fluxes are similar to those shown on the North American Heat Flow Map (http://www.smu.edu/geothermal/2004NAMap/2004NAmap.htm).

The geothermal energy content of the mine water was estimated by summing the energy associated with each flooded underground section, using the following expression for the energy (E_r) of a given section:

$$E_r = Vz\alpha\rho_w Cp_w \quad (6)$$

where the calculated volume of water in a mine section (V) and its average depth (z) were used. Eq. (6) assumes that the heat exchanger return temperature is equal to the ground surface temperature above the mine section because the measured geothermal gradient (α) is used to establish the temperature difference between the surface and the mine workings; the ground surface temperature is taken from Fig. 4.

The volume of water flooding the mine was estimated by multiplying the area of each excavated section by its average thickness. This volume was then multiplied by a correction factor of 0.25 to account for subsidence, pillars and backfill (Jessop et al., 1995). Table 1 shows the volumes calculated for each underground section, which, combined, reach a total volume of water flooding the mine on the order of 3.7 million m^3. Using Eq. (6), the energy contained in this volume of water is approximately 6.1×10^{13} J. The C zone alone contains about 60% of all the water in the workings and about 50% of the available energy. Table 1 also reveals that the estimated thermal energy content of an underground section greatly depends on its depth. For example, the deep section E-32 and the shallow section B-east contain similar water volumes, but the former contains about seven times more energy.

3. Pumping test

A pumping test was conducted at the mine site to quantify the rate at which geothermal energy can be extracted using heat pumps. Additional objectives of the test were to determine

Table 1
Water volume and thermal energy resources contained in underground sections of the Gaspé Mines

Underground section	Average thickness[a] (m)	Area (m^2)	Water volume, V (m^3)	Average depth, z (m)	Energy, E_r (J)
B-east	10	221,200	553,000	100	2.6×10^{12}
C-center	30	297,600	2,232,000	300	3.1×10^{13}
C-northwest	30	8,100	60,750	520	1.5×10^{12}
E-29	34	20,500	174,250	580	4.7×10^{12}
E-32	68	31,400	533,800	670	1.7×10^{13}
E-34	20	21,300	106,500	600	3.0×10^{12}
E-38	20	14,400	72,000	600	2.0×10^{12}
Total		614,500	3,732,300		6.1×10^{13}
$\alpha = 0.011$ °C/m		$\rho_w = 1000$ kg/m^3		$Cp_w = 4225$ J/(kg K)	

Mine working porosity is assumed to be 0.25 to account for subsidence and backfill.
[a] Average thickness from Morin (1992) and Bernard and Procyshyn (1992).

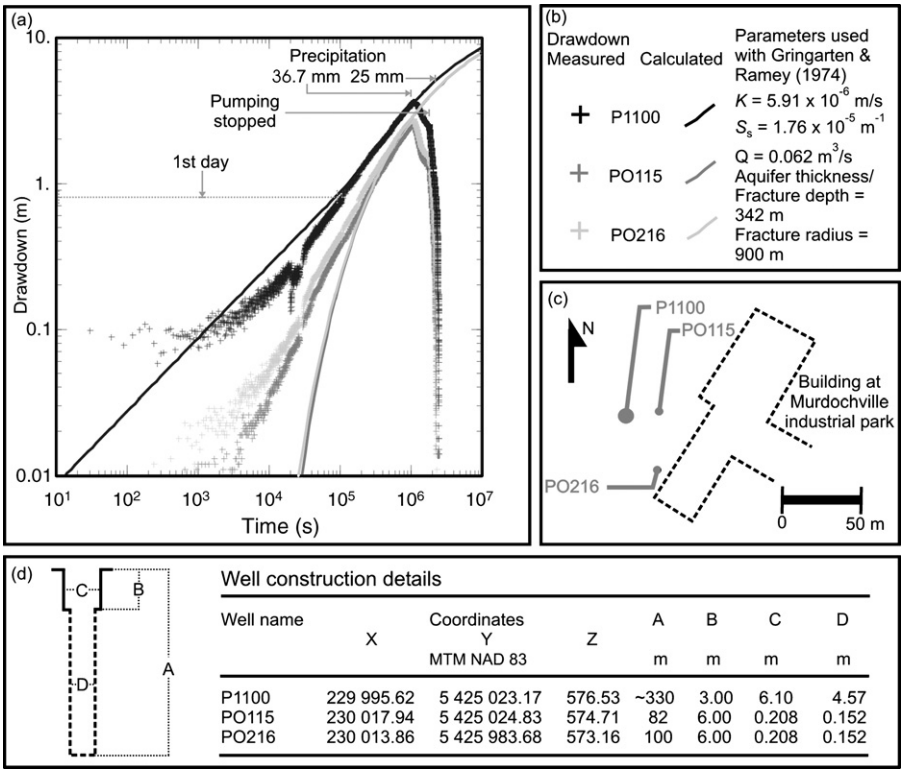

Well construction details

Well name	Coordinates X	Y	Z	A	B	C	D
		MTM NAD 83		m	m	m	m
P1100	229 995.62	5 425 023.17	576.53	~330	3.00	6.10	4.57
PO115	230 017.94	5 425 024.83	574.71	82	6.00	0.208	0.152
PO216	230 013.86	5 425 983.68	573.16	100	6.00	0.208	0.152

Fig. 5. (a) Measured and calculated water table drawdown for the pumping test; (b) analytical solution parameters; (c) location of the pumping well and piezometers; and (d) well construction details.

the mine water chemistry, which can affect the performance of a geothermal system, and the hydraulic properties of the host rock and mine workings; a numerical flow model could then be developed and, together with a simplified energy balance calculation, used to estimate the geothermal potential of the site.

For this test, the old mining shaft referred to in this paper as well P1100 (Fig. 1) was used to pump water at an average rate of 0.062 m^3/s (3720 L/m) for 3 weeks. Converting this mining shaft into a well and installing a 56 kW pump in this roughly 330-m long conduit was a technical challenge because of the geometry of the shaft. It has a diameter of 4.57 m, dips 75° southeast and intercepts the C-central section. The shaft had to be re-opened with a jackhammer because it was cemented at ground surface when the mine closed. Before installing the pump, a steel beam had to be fixed in the shaft with a crane. The pump was then mechanically lowered along the beam to a depth of 49 m. Using the old mining shaft for the pumping test instead of drilling a new well was a less expensive and risky option than drilling a new well as the shaft represented an existing high-capacity, low-cost well.

Two piezometers, PO115 and PO216, were also drilled into the host rock at distances of 22 m east and 43 m south-southeast of P1100, respectively, and were used as observation wells during the test. Construction details and location of the pumping well and the piezometers are shown in Fig. 5c and d. Additional details about the pumping test can be found in Raymond and Therrien (2005).

3.1. Water chemistry

Four water samples were collected at a low-pressure, near-surface valve during the pumping test and were later analysed for alkalinity, hardness, total dissolved solids (TDS) and pH. Total alkalinity was analyzed by titration, total hardness was calculated from Ca and Mg values obtained from chromatographic analyses, and TDS was determined by gravimetric analyses after drying at 180 °C. From these analyses, the calcium carbonate scaling potential was calculated with the Langelier (1936) and Ryznar (1944) saturation indices (LSI and RSI). The saturation pH for calcium carbonate (pH_s) was initially calculated using the following method, described in Rafferty (2000):

$$pH_s = (9.3 + A + B) - (C + D) \tag{7}$$

where

$$A = \frac{\log_{10}(\text{TDS}) - 1}{10} \tag{8}$$

$$B = -13.12 \log_{10}(T_{(K)}) + 34.55 \tag{9}$$

$$C = \log_{10}(\text{hardness}) - 0.4 \tag{10}$$

$$D = \log_{10}(\text{alkalinity}) \tag{11}$$

and where $T_{(K)}$ is the temperature (in K) at which the saturation pH is calculated. The measured pH was then compared to the saturation pH for calcium carbonate for that temperature in order to evaluate the calcium carbonate saturation of the water.

The chemical data (Table 2) indicate that the groundwater is very hard and moderately alkaline. Its pH is slightly higher than that for the pumped water temperature, except for the first sample collected. LSI calculations suggest that the groundwater is slightly oversaturated with respect to calcium carbonate, whereas the RSI values suggest that it is slightly undersaturated. The water is, however, expected to precipitate calcium carbonate during heat pump cooling cycles because the saturation pH decreases with water temperature. Use of resistant and easy-to-clean intermediate

Table 2
Chemical characteristics and calcium carbonate saturation indices for the pumped groundwater sampled in shaft P1100

Saturation index calculation and interpretation	Scaling	Corrosion
$LSI = pH - pH_s$, Langelier (1936)	>0	<0
$RSI = 2pH_s - pH$, Ryznar (1944)	<6	>7

Sampling date	06 October 2005	12 October 2005	19 October 2005	26 October 2005
Pumping day	1	7	14	21
Total alkalinity (mg/L as $CaCO_3$)	81	87	98	98
Total hardness (mg/L as $CaCO_3$)	500	420	400	460
Total dissolved solids (mg/L)	680	710	680	710
pH	7.6	8.0	7.9	7.7
T (°C)	6.6	6.7	6.7	6.8
LSI	−0.13	0.23	0.16	0.02
RSI	7.85	7.54	7.58	7.66

LSI: Langelier saturation index; RSI: Ryznar saturation index.

plate heat exchangers is therefore recommended in order to avoid mineral scaling in the heat exchangers of the heat pumps (Kavanaugh and Rafferty, 1997; Rafferty, 2000). The plate heat exchangers isolate the building water loop and can accommodate incremented load with additional plates.

3.2. Drawdown

Drawdown was measured in the pumping well and the two piezometers with pressure transducers, using Solinst Leveloggers having precisions of 0.02 m in P1100, and 0.01 and 0.005 m in PO115 and PO216, respectively. Water levels in the well and piezometers were also measured during the recovery period, after the end of pumping. Drawdown (Fig. 5a) in the pumping well, shaft P1100, was less then 1 m during the first day of pumping ($t = 8.64 \times 10^4$ s). This small drop in water level after 1 day is explained by the very large dimensions and capacity of shaft P1100, with an important proportion of water initially coming from wellbore (or "shaft") storage. After that first day, drawdown in P1100 kept increasing until it reached a maximum of 3.63 m on the 12th day of pumping ($t = 1.04 \times 10^6$ s). Heavy precipitation on the 11th, 12th and 13th days, with a combined rainfall of 36.7 mm, caused a subsequent water level rise although pumping of the well continued. Pumping was stopped after 21 days ($t = 1.81 \times 10^6$ s) and the water level recovered, reaching its original elevation 7.7 days later; i.e. total time = 28.7 days ($t = 2.48 \times 10^4$ s). A significant snowfall, equivalent to 25 mm of rain, occurred during the first and second days of recovery. All the snow subsequently melted within 4–5 days.

The measured drawdown was used to get an initial estimate of the hydraulic conductivity and specific storage coefficient based on the Gringarten and Ramey (1974) analytical solution for a pumping well that intercepts a horizontal fracture located in an aquifer. The aquifer here is the host rock, which is considered to be homogeneous. Although developed for a single fracture, the solution is applicable here if an analogy is made between a horizontal fracture and horizontal underground workings, which are assumed to behave like a long high-permeability fracture or, equivalently, a preferred path for groundwater flow because of their much higher hydraulic conductivity compared to the host rock. Gringarten and Ramey's (1974) solution is derived for a small diameter well and does not account for wellbore storage effects, which can significantly affect measured drawdown when the pumping well has a large diameter, as is the case here. The solution can nevertheless be used to match late-time (after 1 day) pumping test data, when wellbore storage effects become negligible.

Drawdown calculated with the Gringarten and Ramey (1974) analytical solution was matched to measured drawdown in the pumping and observation wells between the second (i.e. not the first) and 12th day of pumping, times during which it is assumed that there were no storage and boundary effects (Fig. 5a). The match was achieved by specifying a hydraulic conductivity equal to 5.91×10^{-6} m/s (0.61 darcy) and a specific storage coefficient equal to 1.76×10^{-5} m^{-1} for the host rock. This high hydraulic conductivity can be explained by rock fracturing induced by mine blasting. Slug tests performed in PO115 and PO216 (Raymond and Therrien, 2005) gave even higher hydraulic conductivity values for the host rock, equal to 7.75×10^{-5} m/s (8.02 darcy) and 1.12×10^{-4} m/s (11.6 darcy), respectively.

Attempts to match measured drawdown with other analytical solutions, such as those of Theis (1935), Copper and Jacob (1946) and Neuman (1974) were not successful. Water level recovery data could not be matched since the recovery rate was accelerated by precipitations, which are not accounted for by analytical solutions.

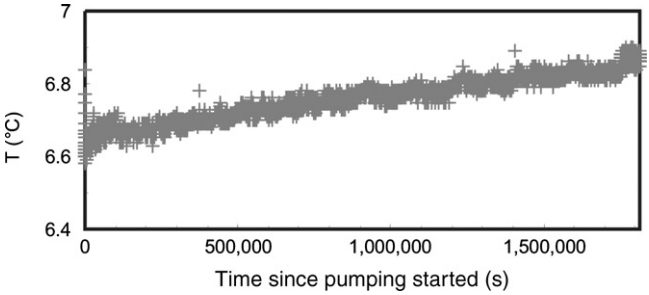

Fig. 6. Pumped water temperature measured at 42 m depth in shaft P1100.

3.3. Temperature and extractable energy rate

The water temperature was measured at a depth of 42 m in pumping well P1100 with a thermistor, using a Solinst levelogger having a precision of 0.1 °C. The flow rate from the well was measured with a pitot flowmeter. The water had a temperature of 6.6 °C at the beginning of the test, which slowly increased to 6.9 °C near the end of the pumping period, with a mean value of 6.7 °C for the test period (Fig. 6).

The geothermal energy rate (E_{hp}) that could be extracted from the pumped water using a heat pump system was calculated from the pumping test data as:

$$E_{hp} = Q(T_p - T_r)\rho_w C p_w \tag{12}$$

where the average values for flow rate (Q) and water temperature (T_p) were used. The heat exchanger return temperature (T_r) was assumed equal to 3 °C, which is the water temperature near the surface of the mine geothermal reservoir. Using Eq. (12), the potential energy production rate from the mine waters is estimated to be 969 kW.

4. Groundwater flow modelling

4.1. Modelling strategies

In order to simulate groundwater flow through a 3D domain, including mine workings, we must first simplify the system of galleries, underground roads and shafts. To reproduce and predict groundwater level recovery mine galleries, underground roads and shafts have been represented using a network of 1D line elements. In these models, pipe flow was computed along 1D elements and the nodal flow contributions for these elements was either transferred to the 3D porous medium flow equation using a fluid transfer term (Adams and Younger, 2001) or added directly to the nodal flow terms corresponding to the 3D elements of the porous medium (Boyaud and Therrien, 2004).

Detailed digital maps of the mine workings were not available for the Gaspé Mines, making their representation by 1D elements a problem. It was also difficult to ascertain the hydraulic connections existing between workings because there was no good record of how the shafts and roads were blocked during closure. The workings were instead represented by broad 3D sub-domains of high hydraulic conductivity geometrically constrained by planar maps of the excavated zones and their relative elevations. Zones that had been mined by the room-and-pillar method were typically left empty and zones that were mined by the longhole method were backfilled. Some of the open spaces may have collapsed as evidenced by land subsidence that occurred over the B-east section.

A homogenous and isotropic value for hydraulic conductivity was used to represent all the mine workings in the absence of detailed records of collapsed/uncollapsed and filled/unfilled workings. The hydraulic conductivity contrast between the workings and the host rock offered a preferred path for groundwater flow that is representatively reproduced through the workings. The resulting method is simpler to implement and can be achieved in the absence of 3D maps of the mining galleries, underground roads and shafts. A similar method was used to simulate heat and mass transport with the TOUGH2 model (Pruess, 1991) for geothermal energy extraction in the workings of a Polish coal mine (Malolepszy, 2003). A 2D zone of high permeability represented those workings, but the model permeability was not validated against field data.

A groundwater flow model of the Gaspé Mines area was constructed to evaluate the energy that can be captured by pumping water from shaft P1100. The modelling strategy consisted of calibrating the model for natural flow conditions and for pumping, adjusting the hydraulic properties and boundary conditions accordingly. Multiple simulations at various pumping rates were subsequently performed to determine the area affected by the pumping well, which was multiplied by the heat flux to estimate the potential rate of energy captured. The extractable energy rate was compared to the captured energy rate and an energy balance calculation was used to evaluate the sustainable energy production rate.

4.2. Governing equations

The 3D finite element simulator HydroGeoSphere (Therrien et al., 2004) was used to simulate the hydraulic response of the Gaspé Mines to the pumping test. One of the characteristics of this numerical code is that it can be used to simultaneously compute 1D pipe flow and 3D porous media flow.

Fully saturated transient fluid flow in the mine workings and the host rock is governed by:

$$-\nabla(q) + \sum \Gamma_{\mathrm{we}} \pm \Gamma_{\mathrm{bo}} = S_{\mathrm{s}} \frac{\partial h}{\partial t} \tag{13}$$

where the fluid flux (q) is given by:

$$q = -K\nabla(h) = -\frac{\rho_{\mathrm{w}} g}{\mu_{\mathrm{w}}} k \nabla(h) \tag{14}$$

The parameter Γ_{we} refers to the volumetric fluid exchange rate between the subsurface domain and wells; the rate between the subsurface domain and the model boundaries is denoted by Γ_{bo}. The storage term on the right-hand side of Eq. (13) depends on the specific storage coefficient (S_{s}) and the hydraulic head (h).

The parameter Γ_{we} is obtained by simultaneously solving 1D pipe flow along the axis of a well, in this case mining shaft P1100, with (Therrien and Sudicky, 2001):

$$-\bar{\nabla}(\pi r_{\mathrm{s}}^2 q_{\mathrm{we}}) \pm Q\delta(l - l') - P_{\mathrm{we}}\Gamma_{\mathrm{we}} = \pi \frac{\partial}{\partial t}\left[\left(\frac{r_{\mathrm{c}}^2}{L_{\mathrm{s}} + r_{\mathrm{s}}^2}\right) h_{\mathrm{we}}\right] \tag{15}$$

where the well fluid flux (q_{we}) depends on the hydraulic conductivity of the well (K_{we}) obtained from the Hagen-Poiseuille formula (Sudicky et al., 1995) and is given by:

$$q_{\mathrm{we}} = -K_{\mathrm{we}}\bar{\nabla}(h_{\mathrm{we}}) = -\frac{r_{\mathrm{c}}^2 \rho_{\mathrm{w}} g}{8\mu_{\mathrm{w}}} \bar{\nabla}(h_{\mathrm{we}}) \tag{16}$$

The 1D gradient operator along the length direction (l) is denoted by $\bar{\nabla}$. The pumping rate (Q) is applied at a location l' in the well screen and $\delta(l–l')$ is the Dirac delta function. The wetted perimeter of the well is denoted by P_{we}. The storage coefficient of the wellbore forming the right-hand side of Eq. (15) depends on the radius of the well screen (r_s) and casing (r_c), the total length of the screen (L_s) and the hydraulic head in the well screen (h_{we}). The shaft P1100 is therefore represented by a 1D axis of finite capacity intercepting the porous medium.

4.3. Simulation domain

A 3D computational mesh with 123,000 nodes (Fig. 7a) covering 12.8 km^2 was generated by stacking 40 layers of 2D triangular elements along the vertical axis. The elevation of the top of the mesh corresponds to surface topography while the bottom was set 350 m below the elevation

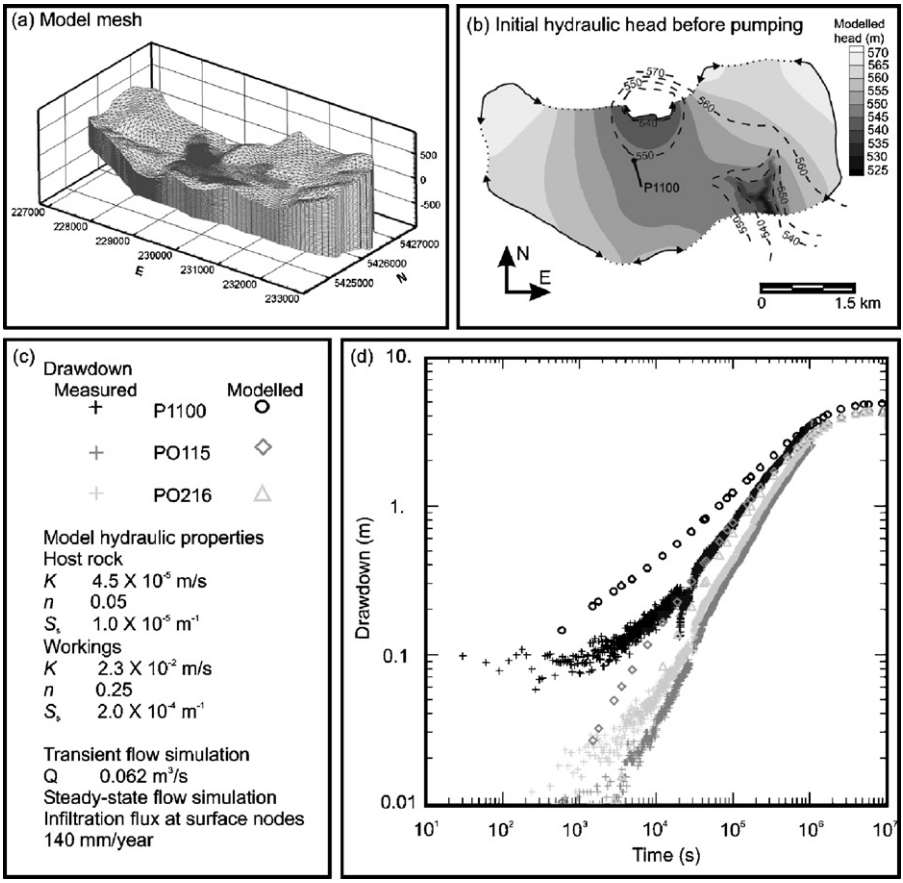

Fig. 7. Model mesh and simulation results obtained during model calibration. (a) Coordinate system (in m) used is the Modified Transverse Mercator NAD83. Legend on the vertical axis shows elevations (m asl). (b) The initial hydraulic heads before pumping shown in plan view were obtained by steady-state fluid flow simulation. The constant head (solid lines with arrows) and impermeable boundaries (dotted lines) and the measured water table elevation (dashed lines) are shown with simulation results. Black dot corresponds to the location of shaft P1100 at ground surface. (c) Model hydraulic properties. (d) Modelled drawdown obtained by transient flow simulation.

of the U2–U3 contact (see Fig. 2), which was well defined from numerous diamond-drilled holes during mineral exploration of the Gaspé Mines. The bottom of the mesh was located deep enough to be considered as an impermeable boundary and minimize its influence on groundwater flow simulated in the mine workings.

Two model sub-domains were created, constrained by the spatial distribution of the host rock and the workings. For each sub-domain, uniform values were used for hydraulic conductivity, porosity and specific storage coefficient. A significantly higher hydraulic conductivity was assigned to the mine working elements compared to the host rock. This simplified approach, which considers the host rock as homogeneous, is assumed to be adequate to model groundwater flow in the mine workings since flow is mainly controlled by the hydraulic conductivity contrast between workings and host rock, as well as by the choice of boundary conditions, which will be discussed next.

The model boundaries were selected according to site elevation (Fig. 3). Topographic highs were assumed to represent recharge areas and were assigned first-type (Dirichlet) boundary conditions with prescribed constant hydraulic head values. The other lateral boundaries perpendicular to equipotentials were assumed to be impermeable. Some uncertainty exists with respect to the choice of boundaries because only a few exploration wells in the study area were available to interpolate water table elevations. A constant hydraulic head value around the Copper Mountain Pit, equal to the elevation of the surface of the water in the pit, was further assigned because it is assumed that pumping at a moderate rate in P1100 has little influence on the pit water level.

All boundaries described above were considered to be uniform with depth such that their values were extended from the surface to the bottom of the mesh. Nodes at the surface that correspond to streams in valleys were assigned a constant head value equal to the surface elevation. The higher parts of the streams were not included in the model because they were assumed to be disconnected from the host rock aquifer. A positive water flux was assigned to the surface nodes to reproduce recharge due to precipitation. With this choice of boundary conditions, water enters the domain from infiltration at the surface with recharge occurring at topographic highs and it leaves the domain at the Copper Mountain Pit and the valley streams.

4.4. Model calibration

The hydraulic properties of the host rock were initially assumed equal to those obtained with the Gringarten and Ramey (1974) solution. Hydraulic properties of the host rock and workings were then modified to match the transient pumping test response. Simulations were performed at a pumping rate of 0.062 m^3/s (3720 L/m) with no infiltration flux at the surface of the domain until the modelled drawdown matched the measured drawdown recorded during the test period that had little or no precipitation (Fig. 7d). Steady-state groundwater flow simulations were subsequently run with an infiltration flux at the surface nodes and no pumpage to adjust first-type boundary conditions at topographic highs.

The steady-state simulations were performed until the modelled drawdown near P1100 matched the measured water table elevation before the pumping test (Fig. 7b). The resulting steady-state hydraulic heads were used as a starting point for further transient pumping test simulations. Steady-state flow and transient pumping were alternatively and repetitively simulated to calibrate the hydraulic properties and adjust the boundary conditions. Calibration was achieved with the constant head boundary values shown in Fig. 3 and by using an infiltration flux equal to 140 mm/year, which is about 13% of the mean precipitation recorded at Murdochville (Environment Canada, 2000). The calibrated hydraulic conductivities and specific storage coefficients for the host rock

Table 3
Captured and extractable thermal energy rates at various pumping flow rates for a 6-month period

Pumping rate, Q (m^3/s)	Affected area (m^2)	Captured energy rate, E_c (kW)	Extractable energy rate, E_{hp} (kW)
0.016	5,720,900	292	250
0.031	6,690,900	341	484
0.049	7,494,600	382	766
0.062	7,904,600	403	969
Heat flux = 51 mW/m^2	$(T_p - T_r) = 3.7$ K	$\rho_w = 1000$ kg/m^3	$Cp_w = 4225$ J/(kg K)

and the underground workings are 4.5×10^{-5} m/s (4.66 darcy), 2.3×10^{-2} m/s (2380 darcy) and 1.0×10^{-5} m^{-1} and 2.0×10^{-4} m^{-1}, respectively.

The calculated drawdown (Fig. 7d) in piezometer PO115 is higher than that observed. The estimated drawdown should be smaller than in PO216, even though PO115 is closer to P1100, because the host rock hydraulic conductivity is anisotropic. The model isotropy introduced a maximum error of 0.4 m in the computed early time drawdown at PO115. The groundwater rebound caused by dewatering that occurred during mining is not considered in the simulations because its effect on drawdown is negligible.

4.5. Captured thermal energy rate

The calibrated model was used for pumping simulations at various rates to determine the area hydraulically affected by the extraction of water from shaft P1100, which is defined as the surface area over the region where drawdown exceeds 1 m. This definition provides a conservative estimate of the area affected by pumping and does not overestimate the potential captured thermal energy rate (E_c). Pumping simulations were conducted for transient flow conditions with no infiltration flux specified at the surface of the domain. These simulations aim to reproduce pumping in winter, when there is no groundwater recharge because the soils are frozen and when groundwater is used for heating. The area affected by pumping was determined for a six-month simulation, which corresponds to the time when flow tends to steady state because no significant changes in hydraulic head are observed after that simulation period. Groundwater is consequently flowing from the constant head boundaries, representing recharge areas, towards the pumping well.

The affected area was multiplied by the surface heat flux to estimate the thermal energy rate that can be captured by pumping in P1100 (Table 3). The rate of energy captured is compared to the potential energy extraction rate computed with Eq. (12). Results of a simulation with a pumping rate of 0.049 m^3/s (2940 L/m) and an affected area of 7,494,600 m^2 are shown in Fig. 8. Calculation of the captured energy rate assumes that groundwater entering the affected area contributes to the heat exchange and can provide thermal energy to the water being produced.

The capture zones of the pumping well were also determined using a particle-tracking algorithm that uses groundwater flow velocities computed from the model; the zones at elevations of 527 and 227 m asl are shown in Fig. 8c and d. Particle tracking suggests that most of the pumped water is tapped from the mine workings because the capture zone is larger at the depth corresponding to the intersection of the pumping well and the C zone (227 m asl) than it is near the ground surface, at the elevation of the pumping node (527 m asl).

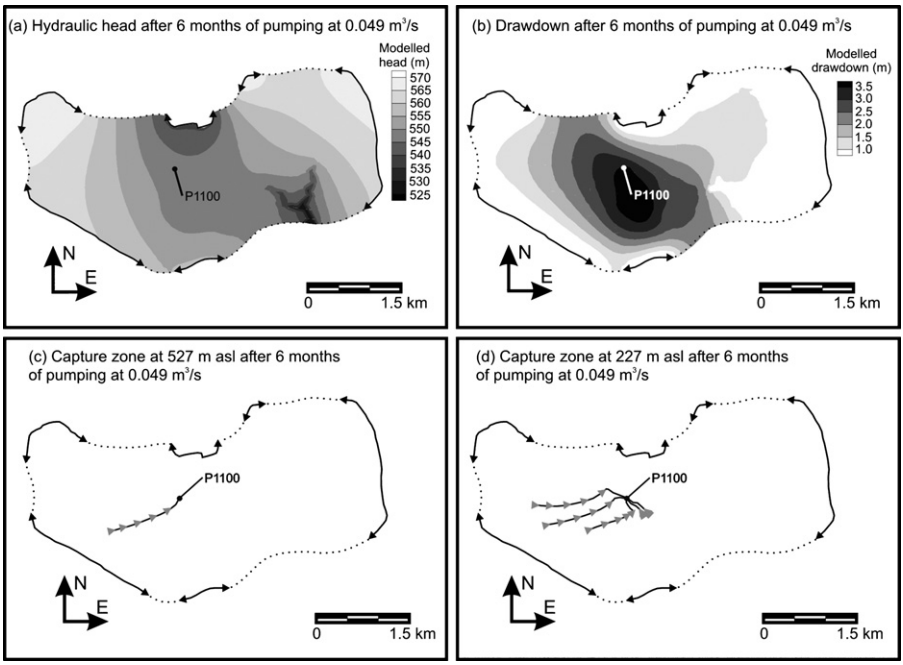

Fig. 8. (a) Modelled hydraulic head, (b) drawdown, and (c and d) capture zones shown in plan view at two different elevations after 6 months of pumping at a rate of 0.049 m^3/s (2940 L/m). Grey triangles in the capture zones are placed at 10-year travel-time intervals. Dots representing shaft P1100 correspond to its location at surface in (a) and (b) and to its location at the elevation of the capture zone in (c) and (d). Constant head (solid lines with arrows) and impermeable boundaries (dotted lines) are shown on the maps.

4.6. Energy balance calculation and geothermal potential

A simplified energy balance calculation was established to estimate the low-temperature geothermal energy extraction potential of the flooded mine. The calculation is done assuming that drawdown caused by the pumping of the mine waters will approach steady state after a heating season. The affected area will consequently remain constant and the flow rate entering the domain at the boundaries will be equal to the pumping rate. For these conditions, the heat recharge to the pumped water is due to the geothermal heat flux over the affected area (i.e. the capture thermal energy rate), by advection from groundwater flowing from the boundaries, and by conduction that can occur when the system starts cooling. If the last two components are neglected, and considering that energy extraction takes place only during half of the year, whereas the geothermal heat flux is continuous, a sustainable energy production rate can be determined by finding the pumping rate at which the captured energy rate (E_c) is half the rate of energy extraction from water by means of heat pumps (E_{hp}). That is:

$$E_{hp} = 2E_c \tag{17}$$

The conditions given in Eq. (17) are reached at a pumping rate of 0.049 m^3/s (2940 L/m), which correspond to an estimated geothermal potential of about 765 kW. This potential energy production can sustain an equivalent peak ground load without significantly cooling water in the reservoirs as pumped water will eventually be injected or replaced by colder surface water. The

potential can be considered as a minimum value because two components of the energy input to the pumped water are neglected.

5. Economic considerations

The geothermal resources of the Gaspé Mines could be used to heat buildings at Murdochville industrial park located near the former mining shaft P1100. A geothermal energy distribution network would be used to transport the pumped mine water to the buildings, which are assumed to be equipped with their own heat pump systems, and to dispose the returned (cooled) water. The point of discharge for this water could be surface water bodies or other mining shafts more than a kilometre east of the pumping well.

An independent economic study (Cavanagh-Morin, 2006) was conducted to evaluate the heating energy savings provided by this energy network. The study assumes a serial pattern for water distribution and return such that the first user benefits from a higher water temperature than the last user. The installation cost of the network of pipelines needed to distribute the geothermal water is estimated at 523,124 $CAN, assuming that buildings are equipped with heat pump systems having a total capacity of 822 kW. The coefficient of performance of the heat pumps used in each building varies from 4.4 to 3.4 depending on the temperature of the water delivered. The heat pumps are assumed to be used in heating mode for 4000 h a year and the total ground load (i.e. load imposed to the subsurface) remains below the geothermal energy extraction potential.

The estimated annual energy required to operate the pumps for the distribution network and all heat pumps are 372.0 and 777.6 MWh, respectively. In comparison, the annual energy required for an oil heating system of an equivalent capacity with 75% efficiency furnaces is 3599 MWh. The economic assessment assumes an average electricity price for the province of Québec in 2006 of 0.06$CAN/kWh for the energy consumed, with a demand charge of 12$CAN/kW and a furnace oil price of 700$CAN/$m^3$. Potential annual savings for users of the geothermal heating system are on the order of 143,600 $CAN. Further details are given in the Cavanagh-Morin (2006) report.

6. Discussion

The geothermal potential estimated in this study corresponds to a minimum energy extraction rate that can be sustained without significantly decreasing the water temperature in the reservoir. The potential is determined from groundwater flow modelling results coupled to simplified energy balance calculations and it is therefore sensitive to the model boundaries and the drawdown limitation, which is assumed equal to 1 m. It also assumes that the geothermal heat flux is the most important energy input to the pumped water.

The sustainable rate of energy production is determined for heating purposes only and would be greater if the analysis were to include space cooling. In such a case, the warmer water returned to the reservoir would increase the energy extraction potential. This scenario has not been considered because the need for cooling in Murdochville is low. The method presented here to calculate the geothermal energy production potential can be applied to other flooded mines to obtain initial estimates in an early project phase. Additional groundwater flow simulations performed with a non-isothermal model taking into account heat exchange governed by advection and conduction could help refine calculation of the geothermal potential. Fluid flow, water level, and temperature data obtained in the early production phase of a project would be useful to validate further simulations.

Because a high pumping rate can be maintained at well P1100, significant heat extraction can be achieved even though the recovered water temperature at the Gaspé Mines is about half that at other documented sites (Jessop et al., 1995; Ghomshei and Meech, 2003; Malolepszy et al., 2005; Watzlaf and Ackman, 2006). The higher temperature at the other sites results from slightly larger heat fluxes, greater mine depths, and/or mineral oxidation. The former factor appears to have an important influence on mine water temperature and may complicate geothermal exploitation in the base-metal mining environment because of associated acid mine water that could damage the heat pump systems. Significant mineral oxidation is believed to be of minor importance at Gaspé Mines because the groundwater is relatively cold and most of the workings are flooded. The calcareous host rock also provides a neutralizing environment that minimizes the formation of acid mine drainage. In contrast, Ghomshei and Meech (2003) reported an effluent water pH on the order of 4–4.5 at the former Britannia Mine, British Colombia, Canada. These authors suggest using special acid-resistant heat exchangers to cope with mine effluents. Fortunately, the absence of acid mine drainage at the Gaspé Mines will facilitate geothermal operations.

The Gaspé Mines are characterized by an elevated hydraulic conductivity enhanced by the network of mine workings. Modelling results indicate that the workings equivalent hydraulic conductivity is about to 2.3×10^{-2} m/s (2380 darcy), similar to that of gravel aquifers. Workings at other flooded mines should have a similar hydraulic conductivity and can therefore be considered for geothermal heating using heat pumps even though they may be located in an area of low surface heat flux such as the Canadian Shield and the Appalachians (Jessop et al., 1984). The results of this study, combined with the inventory of inactive mines compiled by Arkay (1992) and the geothermal research work outlined in Jessop et al. (1991), Allen et al. (2000) and Ghomshei et al. (2005) suggest that geothermal energy extraction can be undertaken at most of the flooded Canadian mines where there is need for heating.

7. Conclusions

The 3.7 million m^3 of water flooding the Gaspé Mines can be exploited to extract some of the 6.1×10^{13} J of thermal energy stored in the workings. The old mining shaft P1100 could be used to produce mine waters at a rate greater than needed to exploit the site's geothermal potential. The 6.7 °C mine water pumped at a rate of 0.049 m^3/s (2940 L/m) could be used with heat pumps to lower the water temperature to 3 °C and extract geothermal energy at a rate of 765 kW.

Groundwater flow modeling and the energy balance calculation suggest that this energy production rate could be sustained without significantly affecting the water temperature in the flooded mine workings. Intermediate plate heat exchangers are recommended for use with the alkaline mine water to isolate the building loop and avoid the mineral scaling in the heat exchangers of the heat pumps that can occur during cooling cycles.

This study allowed us to characterize the complex low-temperature geothermal reservoir formed by the flooded Gaspé Mines. Calibration of the finite-element model used to reproduce the hydraulic response of a pumping test performed in a former mining shaft proved an efficient method for determining the equivalent hydraulic properties of the mine workings. Model drawdown predictions helped to estimate the energy rate that can be captured by the pumping well. Finally, the geothermal potential of the mine site was estimated with a simplified energy balance calculation. The method used here can rapidly lead to a confident assessment of the geothermal potential of a mine site within the context of a feasibility study. Based on the results of this

preliminary study, a geothermal energy distribution network designed for the industrial park of Murdochville, located over the mine workings, could be constructed to supply the water needed to heat the industrial buildings in an economical manner.

Acknowledgements

The authors would like to thank the authorities and population of the town of Murdochville for their collaboration and financial support during this study. The collaboration of Murdochville Economic Diversification Committee, Murdochville Chamber of Commerce and Tourism, and the Gaspé Mines personnel at Xstrata is also acknowledged. Additional funding was provided by the Fonds québecois de la recherche sur la nature et les technologies (FQRNT) and by the Natural Sciences and Engineering Research Council of Canada (NSERC). Comments from Dr. René Lefebvre, Philippe Chevrier and the journal editors greatly helped to improve the manuscript.

References

Adams, R., Younger, P.L., 2001. A strategy for modeling ground water rebound in abandoned deep mine systems. Ground Water 39, 249–261.

Allcock, J.B., 1982. Skarn and porphyry copper mineralization at Mines Gaspé, Murdochville, Quebec. Econ. Geol. 77, 971–999.

Allen, D.M., Ghomshei, M.M., Sadler-Brown, T.L., Dakin, A., Holtz, D., 2000. The current status of geothermal exploration and development in Canada. In: Proceedings of the World Geothermal Congress, Kyushu-Tohoku, Japan, May 28–June 10, pp. 55–58.

Arkay, K., 1992. Geothermal energy from abandoned mines: a methodology for an inventory, and inventory data for abandoned mines in Québec and Nova Scotia. Open file report 3825. Geological Survey of Canada, Alberta, 45 pp.

Banks, D., Younger, P.L., Arnesen, R.-T., Iversen, E.R., Banks, S.B., 1997. Mine-water chemistry: the good, the bad and the ugly. Environ. Geol. 32, 157–174.

Bernard, P., Procyshyn, E.L., 1992. Geology and Mineral Exploration at Mines Gaspé. In: Proceedings of the 94th CIM Annual Meeting, Montréal, Canada, April 26–30, pp. 111–115.

Boyaud, C., Therrien, R., 2004. Numerical modeling of mine water rebound in Saizerais, northeastern France. In: Miller, C.T., Farthing, M.W., Gray, W.G., Pinder, G.F. (Eds.), Computational Methods in Water Resources. Developments in Water Science, 55, vol. 2. Elsevier, Amsterdam, The Netherlands, pp. 977–989.

Brailsford, A.D., Major, K.C., 1964. The thermal conductivity of aggregates of several phases, including porous materials. J. App. Phys. 15, 313–319.

Cavanagh-Morin, G., 2006. Évaluation économique projet géothermie Mines Gaspé. Unpubl. report, Les Services Technologiques Duo, Gaspé, Canada, 17 pp.

Chemical Rubber Company, 2006. CRC Handbook of Chemistry and Physics. Available on the Internet at: http://www.hbcpnetbase.com.

Clauser, C., Huenges, E., 1995. Thermal conductivity of rocks and minerals. In: Ahrens, T.J. (Ed.), Rock Physics and Phase Relations: A Handbook of Physical Constants, AGU Reference Shelf, vol. 3. American Geophysical Union, Washington, DC, USA, pp. 105–126.

Copper, H.H., Jacob, C.E., 1946. A generalized graphical method for evaluating formation constants and summarizing well field history. Am. Geophys. Union Trans. 27, 526–534.

Drury, J.M., Jessop, A.M., Lewis, T.J., 1987. The thermal nature of the Canadian Appalachian crust. Tectonophysics 133, 1–14.

Environment Canada, 2000. Murdochville Climate Normals 1971-2000. Available on the Internet at: http://www.climat.meteo.ec.gc.ca/climate_normals/index_e.html.

Freeze, R.A., Cherry, J.A., 1979. Groundwater. Prentice-Hall, Englewood Cliffs, NJ, USA, pp. 604.

Geocon, 1994. Unité 7-Méthodes d'exploitation. Caractérisation environnementale du site de Mines Gaspé. Unpubl. report, SNC Lavalin, Shawinigan, Canada, 10 pp.

Geothermal Heat Pump Consortium, 1997. Municipal Building, Park Hills, Missouri. Available on the internet at: http://www.geoexchange.org/pdf/cs-064.pdf.

Ghomshei, M.M., Meech, J.A., 2003. Usable heat from mine waters: coproduction of energy and minerals from "Mother Earth". Proceedings of the Fourth IPMM Conference, Sendai-Matsushima, Japan, May 18–23, p. 8.

Ghomshei, M.M., MacLeod, K., Sadlier-Brown, T.L., Meech, J.A., Dakin, R.A., 2005. Canadian geothermal energy poised for takeoff. In: Proceedings of the World Geothermal Congress 2005. Antalya, Turkey, April 24–29, Paper 0158, 4 pp.

Gringarten, A.C., Ramey, H.J., 1974. Unsteady-state pressure distributions created by a well with a single horizontal fracture, partial penetration, or restricted entry. Soc. Petrol. Eng. J. 14, 413–426.

Huttrer, G.W., 1997. Geothermal heat pumps: an increasingly successful technology. Renew. Ener. 10, 481–488.

Jessop, A.M., Lewis, T.J., Judge, A.S., Taylor, A.E., Drury, M.J., 1984. Terrestrial heat flow in Canada. Tectonophysics 103, 239–261.

Jessop, A.M., Ghomshei, M.M., Drury, M.J., 1991. Geothermal energy in Canada. Geothermics 20, 369–385.

Jessop, A.M., MacDonald, J.K., Spence, H., 1995. Clean energy from abandoned mines at Springhill, Nova Scotia. Ener. Sources 17, 93–106.

John Gilbert Architects, 2006a. Sustainable housing, Glenalmond Str. Available on the internet at: http://www.johngilbert.co.uk/pdf_files/innovation/9_Shettleston.pdf.

John Gilbert Architects, 2006b. A technical report on Ochil View, Lumphinnans. Available on the internet at: http://www.johngilbert.co.uk/pdf_files/JGA_Lumphinnans_tech.pdf.

Kavanaugh, S.P., Rafferty, K., 1997. Ground-source heat pumps: design of geothermal systems for commercial and institutional buildings. In: Proceedings of the American Society of Heating Refrigerating and Air-Conditioning Engineers, Atlanta, GA, USA, pp. 72–73.

Langelier, W.R., 1936. The analytical control of anti-corrosion water treatment. J. Am. Water Work Assoc. 28, 1500–1521.

Malolepszy, Z., 2003. Low-temperature, man-made geothermal reservoirs in abandoned workings of underground mines. In: Proceedings of the 28th Workshop on Geothermal Reservoir Engineering, Stanford University, Stanford, CA, USA, pp. 259–265.

Malolepszy, Z., Demollin-Schneiders, E., Bowers, D., 2005. Potential use of geothermal mine water in Europe. In: Proceedings of the World Geothermal Energy Congress 2005, April 24–29, Antalya, Turkey, Paper 0254, 3 pp.

Morin, G., 1992. Exploitation des mines. Unpubl. report Minéraux Noranda Inc. Mines Gaspé Division. Murdochville, Canada, pp. 18.

Neuman, S.P., 1974. Effect of partial penetration on flow in unconfined aquifers considering delayed gravity response. Water Resour. Res. 10, 303–312.

Pruess, K., 1991. TOUGH2—a general purpose numerical simulator for multiphase fluid and heat flow. Lawrence Berkeley Laboratory report LBL-29400, Berkeley, CA, USA, 102 pp.

Rafferty, K., 2000. Scaling in geothermal heat pump systems. Geo-Heat Center Quart. Bull. 21, 11–15.

Raymond, J., Therrien, R., 2005. Estimation du potentiel de production d'énergie géothermique des Mines Gaspé à Murdochville : essai de pompage. Unpubl. report, Comité de relance de la ville de Murdochville, Murdochville, Canada, 25 pp.

Raymond, J., Therrien, R., 2006. Investigating the low-temperature geothermal potential of the Gaspé Mines, Murdochville, Canada. Geotherm. Resour. Council Trans. 30, 565–569.

Ryznar, J.W., 1944. A new Index for determining amount of calcium carbonate scale formed by water. J. Am. Water Work Assoc. 36, 472–483.

Somerton, W.H., 1992. Thermal properties and temperature-related behavior of rock/fluid systems. Elsevier, Amsterdam, The Netherlands, pp. 275.

Sudicky, E.A., Unger, A.J.A., Lacombe, S., 1995. A noniterative technique for the direct implementation of well bore boundary conditions in three-dimensional heterogenous formations. Water Resour. Res. 32, 411–415.

Theis, C.V., 1935. The relation between the lowering of the piezometric surface and the rate and duration of a well using groundwater storage. Am. Geophys. Union Trans. 16, 519–524.

Therrien, R., Sudicky, E.A., 2001. Well bore boundary conditions for variably saturated flow modeling. Adv. Water Res. 24, 195–201.

Therrien, R., McLaren, R.G., Sudicky, E.A., Panday, S.M., 2004. HydroGeoSphere. In: A Three-dimensional Numerical Model Describing Fully integrated Subsurface and Surface Flow and Solute Transport. Users Manual. Université Laval, University of Waterloo, Canada, p. 300.

Tóth, A., Bobok, E., 2007. A prospect geothermal potential of an abandoned copper mine. In: Proceedings of the 32nd Workshop on Geothermal Reservoir Engineering, Stanford, CA, USA. Stanford University, p. 3.

Waples, D.W., Waples, J.S., 2004a. A review and evaluation of specific heat capacities of rocks, minerals, and subsurface fluids. Part 1. Minerals and nonporous rocks. Nat. Resour. Res. 13, 97–122.

Waples, D.W., Waples, J.S., 2004b. A review and evaluation of specific heat capacities of rocks, minerals, and subsurface fluids. Part 2. Fluids and porous rocks. Nat. Resour. Res. 13, 123–130.

Wares, R., Berger, J., 1993. Stratigraphie, structure et lithogéochimie de la région de Mines Gaspé. Unpubl. report, IXION Research Group, Montréal, Canada, 34 pp.

Wares, R., Berger, J., 1995. Contrôle structuraux des gisements cuprifères de Mines Gaspé. Unpubl. report, IXION Research Group, Montréal, Canada, 31 pp.

Wares, R., Brisebois, D., 1998. Geology and metallogeny of the Cu-porphyry-related Mines Gaspé, Murdochville, Gaspésie. In: Field Trip B4 Guide Book Mineralogical Association of Canada Joint Annual Meeting, Québec, Canada, p. 24.

Watzlaf, G.R., Ackman, T.E., 2006. Underground mine water for heating and cooling using geothermal heat pump systems. Mine Water Environ. 25, 1–14.